Proceedings of the ASME 2010 3rd Joint US-European Fluids Engineering Summer Meeting and 8th International Conference on Nanochannels, Microchannels, and Minichannels
FEDSM-ICNMM2010
August 1-5, 2010, Montreal, Canada

FEDSM-ICNMM2010-30457

AN EFFECT OF SWEPT VANE IN HYDROGEN-FUELED COMBUSTION TURBINE

Hironori HONDA
Department of Mechanical Engineering, Tokyo University of Science, Tokyo, Japan
j4506076@yahoo.co.jp

Masaya SUZUKI
Department of Mechanical Engineering, Tokyo University of Science, Tokyo, Japan
masaya@rs.kagu.tus.ac.jp

Makoto YAMAMOTO
Department of Mechanical Engineering, Tokyo University of Science, Tokyo, Japan
yamamoto@rs.kagu.tus.ac.jp

ABSTRACT

A lot of environmental problems such as global warning, air pollution and exhaustion of fossil fuels have been discussed frequently. Many researches have been underway in several countries to develop a propulsion system for an advanced aircraft to achieve low environmental loading. On the other hand, with the recent development of an aircraft, the propulsion system is required to have lighter weight, higher power and lower emissions. To satisfy these requirements, we have supposed a new cycle concept for advanced propulsion system, in which the combustion camber is eliminated; hydrogen gas is directly injected from turbine vane surfaces and combusted within turbine vane passages. However, to apply the cycle to practical use, there are problems of extremely high surface temperature and aerodynamic performance decrease by hydrogen combustion. It is well known that three-dimensional design approaches such as sweep, lean and twist decrease the secondary flow loss. However, there is no knowledge how these three-dimensional designs affect on the flow characteristics of the hydrogen-fueled turbine. In the present study, we focus on sweep. To clarify the sweep effect on the surface temperature and performance of the hydrogen-combustion turbine, three-dimensional numerical simulations based on RANS are carried out. We find that the swept vanes with positive sweep give the aerodynamic performance. On the other hand, the swept vanes with negative sweep suppress the vane surface temperature.

INTRODUCTION

In these years, global environmental problems become so serious. A lot of environmental problems such as global warning, air pollution and exhaustion of fossil fuels have been discussed frequently. Therefore, low environmental loading is an important requirement for any machines. Many researches have been underway in several countries to develop a propulsion system for an advanced aircraft to satisfy the requirement. Among them, a hydrogen-fueled propulsion system has been researched as a substitute for existing jet-engine systems [1-4]. Hydrogen gas has higher energy per unit weight than conventional hydrocarbon fuels, and has better cooling characteristics than air. Furthermore, it is beneficial that hydrogen burning does not generate SO_x and CO_2 emissions which are the main reason of global warming and air pollution. Besides these advantageous points, we can also clear up the exhaustion problem of fossil fuels by using hydrogen as aircraft fuel.

On the other hand, with the recent development of an aircraft, the propulsion system is required to be lighter. To satisfy the requirement, we have proposed a new cycle concept for advanced propulsion system, in which the combustion camber is eliminated; hydrogen gas is directly injected from turbine blade/vane surfaces and combusted within the flow passages. Nagumo et al.[5] proposed this new cycle concept and proved that this concept can be promising for the realization. In addition, they performed three-dimensional computations of the flow field with chemical reactions of hydrogen combustion within a first stator cascade [6]. Since the combustion process does not complete in the stator passage, to estimate the stage performance, Sato et al. performed three-dimensional computation of rotor/stator interaction with hydrogen combustion [7]. From their results, they concluded that the realizability of this cycle concept has the highest possibility by employing the hydrogen injection rate of $2H_2/O_2 = 0.25$.

However, for the practical use, there exist further problems that must be overcome. In the previous studies, we found that the aerodynamic performance of the blade is largely decreased due to the fuel injection [5-7]. For the purpose of realizing our concept, turbine blade is required to have the adequate performance even with hydrogen injection. Therefore, the blade shape and injector layout optimizations for two-dimensional

turbine blade were carried out to improve the aerodynamic performance of the blade [8]. Ikeda et al. [9] clarified the influence of the injector holes layout on the flow field and the vane surface temperature by three-dimensional simulation within a stator cascade. Miyama et al. [10] investigated the relation between the injector layout and tip leakage flow. They found that high-temperature region is formed on the blade surface near the tip gap and outer casing by combusting tip leakage flow. Although the optimizations improve the turbine performance, it was not sufficient for the advanced low environmental loading engines.

On the other hand, three-dimensional design is more important for practical applications since secondary flow leads significant loss in turbine cascades. It is well known that three-dimensional design approaches such as sweep, lean and twist, decrease the secondary flow loss [11][12]. Hence, it is expected that three-dimensional design improve the aerodynamic performance of the hydrogen-fueled turbine. However, there is no knowledge how these three-dimensional designs affect on the flow characteristics of the hydrogen-fueled turbine. In the present study, we focus on sweep: an effect of swept vane in hydrogen-fueled combustion turbine in terms of the hydrogen mole distribution, surface temperature and aerodynamic performance is investigated. It is clarified that the swept vanes with a positive sweep angle give the aerodynamic performance because the secondary flow is restrained. On the other hand, the swept vanes with a negative sweep angle suppress the vane surface temperature because the secondary flow is promoted and the expansion is late.

NOMENCLATURE

C_L	lift coefficient
C_p	surface pressure coefficient
D_j^m	diffusion coefficient
h_j	specific enthalpy of species j
j_{jk}	diffusion flux of species j in direction k
p	static pressure
P_s	static pressure on vane surface
P_{t1}	inflow total pressure
P_{s2}	outflow static pressure
q_k	heat flux in direction k
t	time
u_i	velocity component in direction i
w_j	production rate for species j
x_i	Cartesian coordinate in direction i
Y_j	mass fraction of species j
δ_{ij}	Kronecker delta
ρ	density of fluid
τ_{ik}	k directional flux of i directional momentum

GOVERNING EQUATIONS

The flow field is assumed to be three-dimensional, turbulent and with chemical reactions. Therefore, the Reynolds-averaged compressible Navier-Stokes equations and species transport equations for the chemically reacting gas are employed as the governing equations. The turbulence model is the high-Reynolds-number type k-epsilon model proposed by Launder-Spalding [13]. These equations are expressed as follows;

$$\frac{\partial \overline{\rho}}{\partial t} + \frac{\partial}{\partial x_k}\left(\overline{\rho}\widetilde{u}_k\right) = 0 \tag{1}$$

$$\frac{\partial \overline{\rho}\widetilde{u}_i}{\partial t} + \frac{\partial}{\partial x_k}\left(\overline{\rho}\widetilde{u}_i\widetilde{u}_k + \overline{p}\delta_{ik}\right) = \frac{\partial}{\partial x_k}\left(\overline{\tau}_{ik} - \overline{\rho u_i^{"} u_k^{"}}\right) \tag{2}$$

$$\begin{aligned}\frac{\partial \overline{\rho}\widetilde{e}}{\partial t} + \frac{\partial}{\partial x_k}\left(\overline{\rho}\widetilde{e}\widetilde{u}_k + \overline{p}\widetilde{u}_k\right) \\ = \frac{\partial}{\partial x_k}\left(\overline{\tau}_{ik}\widetilde{u}_i - \overline{q}_k - \sum_{j=1}^{n}\overline{j_{jk}h_j} - \overline{\rho u_k^{"} h^{"}}\right)\end{aligned} \tag{3}$$

$$\frac{\partial \overline{\rho}\widetilde{Y}_j}{\partial t} + \frac{\partial}{\partial x_k}\left(\overline{\rho}\widetilde{Y}_j\widetilde{u}_k\right) = -\frac{\partial}{\partial x_k}\left(j_{jk} + \overline{\rho u_k^{"} Y_j^{"}}\right) + \overline{w}_j \tag{4}$$

$$(j = 1,2,\cdots,n)$$

where Y_j, j_{jk}, w_j and h_j denote the mass fraction, the diffusion flux in k-direction, the chemical rate of production per unit volume, and the specific enthalpy of species j, respectively. In the diffusion flux of species j, we consider only the diffusion by the concentration gradient and it can be expressed with the diffusion coefficient D_j^m by next equation;

$$j_{jk} = -\overline{\rho}D_j^m\frac{\partial \widetilde{Y}_j}{\partial x_k} \tag{5}$$

In Eqs. (2) to (4), $-\overline{\rho u_i^{"} u_k^{"}}$, $\overline{\rho u_k^{"} h^{"}}$ and $\overline{\rho u_k^{"} Y_j^{"}}$ are described by the Boussinesq and gradient diffusion hypotheses;

$$-\overline{\rho u_i^{"} u_k^{"}} = \mu_t\left(\frac{\partial \widetilde{u}_i}{\partial x_k} + \frac{\partial \widetilde{u}_k}{\partial x_i} - \frac{2}{3}\frac{\partial \widetilde{u}_l}{\partial x_l}\delta_{ik}\right) \tag{6}$$

$$\overline{\rho u_k^{"} Y_j^{"}} = -\overline{\rho}D_{jt}\frac{\partial \widetilde{Y}_j}{\partial x_k} \tag{7}$$

$$\overline{\rho u_k^{"} h^{"}} = -\frac{\lambda_t}{C_p^m}\frac{\partial \widetilde{h}}{\partial x_k} \tag{8}$$

In the above equations, D_{jt} and C_p^m are given by using Schmidt and Prandtl numbers;

$$D_{jt} = \frac{\mu_t}{\overline{\rho}\sigma_{jt}} \tag{9}$$

$$C_p^m = \frac{\sigma_{ht}\lambda_t}{\mu_t} \tag{10}$$

where both σ_{jt} and σ_{ht} are assumed to be unity. After verifying the chemical reaction models proposed by Huang-Chen [14], Balakrishnan-Williams [15], Sanchez et al. [16] and Chen et al.

Table 1 5-step reduced mechanism by Chen et al.

1	$O_2 + H$	⇔	$OH + O$
2	$H_2 + O$	⇔	$H + OH$
3	$H_2 + OH$	⇔	$H + H_2O$
4	$H + O$	⇔	OH
5	$O_2 + N_2$	⇔	$2NO$

[17], 5-step reduced mechanism model proposed by Chen et al. [17] is applied for the source term in the species transport equations. The reason why we choose this model is that it has high predictability, stability and light computational load. Table 1 shows the 5-step reduced mechanism model. This model takes 8 species; H_2, O_2, H_2O, N_2, H, O, OH and NO. The thermodynamic properties (e.g. enthalpy and specific heat) are expressed as a function of species and temperature from JANAF data [18].

NUMERICAL PROCEDUARES

As the numerical procedures, we employ a finite difference method. In combustion process, the elementary reactions have greatly different time-scales, and so that stiffness problem between time-scales of the fluid flow and the chemical reactions occurs in the computations. Therefore, point implicit method is adopted for the time integration. The chemistry source terms are implicitly calculated by Crank-Nicolson method and other terms are explicitly estimated by 2-stage Runge-Kutta method. For the spatial differences, considering the numerical stability and accuracy, 2nd-order upwind TVD scheme proposed by Yee-Harten [19] is employed for the inviscid terms, and 2nd-order central differencing scheme is adopted for the other terms.

COMPUTATIONAL CONDITIONS

The vane profile and the cascade geometry are quoted from the reference literature [20]. The computational geometry and jet parameters are given in Table 2. The chord length is 31.80 mm, the pitch is 23.09 mm, the span length is 24.60 mm, the inflow angle is 0 deg, and the stagger angle is 47.50 deg. Since the flow field in a stator is simple because of no rotation effect and leakage vortex, the present computations are carried out for only the stator neglecting stator-rotor interaction.

Figure 1 illustrates schematic diagram of the turbine cascade and the computational grids used in this study. With the main grid, the calculations for the flow field within a turbine vane passage are conducted. With Sub Grid, which is O-type grid fitted around the vane, boundary layer over the turbine vane is evaluated. It is noted that the overlapping data are interpolated linearly. A certain amount of grid points are clustered near the vane wall and endwall. The number of total grid points is approximately 510,000.

In this study, we decided the flow conditions on the basis of the cycle analysis of the GE90 engine under the taking-off condition at sea level. High-pressure air which passes through the HP compressor flows directly into the first stage of the HP turbine due to the elimination of the combustor. At the HP compressor exit, the total temperature and the total pressure of air are 903.42 K and 3.92 MPa, respectively. Then the flow expands to static pressure 3.36 MPa at the outflow boundary of the computational domain. The displacement thickness at the inflow boundary of the computational domain is set to 1% of overall flow rate.

Hydrogen is injected from the stator surface as the gaseous fuel. The area of a jet injector is 73.80 mm^2. Injection area is allocated around the leading edge as illustrated in Fig. 2. The static temperature of hydrogen is fixed to be 900 K, and the direction of injection is normal to the vane surface. The total mass flow ratio of hydrogen to inflow air is a quarter of stoichiometric ratio. Sato et al. [7] proved that this hydrogen injection rate has high realizability of this cycle concept. Nine cases are computed: namely S0, S15, S30, H2S0, H2S15, H2S30, H2CS0, H2CS15 and H2CS30. S0, S15 and S30 mean the sweep angles are 0, 15 and 30 deg., H2 denotes the hydrogen injection and C signifies combustion.

Table 2 Stator specifications

Chord length	31.80	[mm]
Pitch length	23.09	[mm]
Span length	24.60	[mm]
Inlet angle	9.75	[deg.]
Exit angle	37.75	[deg.]

RESULTS AND DISCUSSION

First, to understand the fundamental flow field around the swept vane, the characteristics of the flow field without hydrogen injection are examined.

Figure 3 shows the streamlines at the sweep angle 30 deg., S30. The streamlines near the suction and pressure surfaces are shown in Fig. 3 (a) and (b), respectively. The tip endwall is top and the hub endwall is bottom. The free-stream flows from the right side in Fig.3(a) and from the left side in Fig.(b), respectively. The spanwise flow does not occur in the straight vane. However, in the swept vane, streamlines deflect from the hub to the tip around the leading edge, because the leading edge of the hub is closer to the inlet than the tip, and so the spanwise pressure gradient occurs. Similarly, the spanwise pressure gradient due to the delay of expansion at the tip deflects the streamlines from the tip to the hub around the trailing edge.

To clear the static pressure distributions near the endwalls, Figs. 4 and 5 show the distributions of vane surface pressure coefficient C_p at 5% span from the hub and tip, respectively. Surface pressure coefficient C_p is defined as follows;

$$C_p = \frac{P_s - P_{s2}}{P_{t1} - P_{s2}} \tag{11}$$

In the pictures, the axis of ordinate shows C_p and the axis of abscissa shows the dimensionless x direction normalized by the axial chord length. The x direction is shown in Fig. 2. Comparing the distributions for the swept vane and the straight one (i.e. S0), the following insights were obtained. The static pressure increases near the hub and decreases near the tip for larger sweep angle. The pressure differences between the suction side and the pressure side decreases near the hub and increases near the tip. By the spanwise pressure differences, the secondary flow from the pressure side to the suction side is restrained near the hub and promoted near the tip. The another secondary flow from the hub to the tip is generated at both of the pressure and suction sides Although the spanwise direction of this secondary flow changes reversely along the axial

position, the sweep effect is stronger around the leading edge than the trailing edge, and so the secondary flow has the direction from the hub to the tip until the considerably downstream region. There is extremely small difference between with and without hydrogen injection because hydrogen is a little and much lighter than air.

Next, to see the vortex structure due to the secondary flow, Fig. 6 show the streamlines visualized by line integral convolution (LIC) method at 90% chord. The results are shown for three cases: sweep angle is 0, 15 and 30 deg. without hydrogen injection. The top is the tip and the bottom is the hub in the figure. In the case of the straight vane, S0, there is secondary flow near both sides of the endwalls. Comparing the straight vane to the swept vanes, the swept vanes restrain the secondary flow near the hub and promote it near the tip because the pressure gradient from the pressure surface to the suction surface decreases near the hub and increases near the tip by the vane sweep. As not shown here, these trends are same as the cases with hydrogen injection and combustion.

Figures 7 and 8 show the enlarged view of streamlines near the tip and the hub, respectively. From the results, it is clear that the secondary flow generates passage vortexes. The passage vortex near the tip is expanded and leaves the endwall due to the sweep. While the passage vortex near the hub becomes small and closes to the endwall.

For evaluation of turbine performance, we discuss total pressure distributions. Figure 9 shows the total pressure distributions at the trailing edge. The results of six cases are exhibited: the upper and lower pictures are the cases with and without hydrogen injection, respectively; the left, middle and right ones are the sweep angle of 0, 15 and 30 deg., respectively. From these figures, the total pressure loss decreases at the hub and increases at the tip by swept effect because the secondary flow is suppressed near the hub and promoted near the tip by the change of the static pressure distributions. The area of total pressure loss is a little larger in the case with hydrogen injection than the case without hydrogen injection because the velocity near the wall surface is accelerated by hydrogen injection. In the present computations, we use the swept vanes which have positive sweep angle at the hub and negative sweep angle at the tip. From the numerical results, we can make an inference that swept vanes with a positive sweep angle at both of the hub and tip decreases effectively the total pressure loss because of the weakened secondary flow near the both endwalls.

The results about the sweep effect as mentioned above agree with the existing studies without hydrogen injection [11][12]. The influence of sweep in the case with hydrogen injection is similar to the case without hydrogen injection. However, the significant results of the present study are the relation between the sweep and hydrogen combustion. From the next paragraph, the influence of sweep on hydrogen combustion is discussed.

Figures 10 and 11 exhibit the hydrogen mole fraction distributions on the vane surface and the trailing edge, respectively. The top, middle and bottom results in Fig.10 are respectively H2S0, H2S15 and H2S30. The point of view in Fig. 10 is same as that in Fig. 3. The results of left, middle and right in Fig.11 are respectively H2S0, H2S15 and H2S30. The point of view is same as that in Fig. 9. From these figures, it is clear that the secondary flow affects hydrogen mole distribution. The hydrogen mole fraction increases near the hub and decreases near the tip since spanwise flow is restrained near the hub and promoted near the tip, as mentioned above. The spanwise distribution of the hydrogen mole fraction on the pressure surface is uniform, while the distribution around the suction side is not uniform.

Figure 12 shows the static temperature distribution on the suction surface of the vane. The left, middle and right results in this figure are respectively H2CS0, H2CS15 and H2CS30. The point of view in Fig. 12 is same as that in Fig.3(a). From this figure, it can be confirmed that combustion does not occur within the secondary flow core, and the high temperature is found in the surroundings of the vortex. This is thought that there is no hydrogen in the secondary flow core from Fig.10, and combustion is promoted by mixing hydrogen with oxygen around the interface between the secondary flow and the main stream. From our previous researches, it is known that hydrogen combustion is remarkably promoted by high temperature. The temperature near the hub rises, compared with the tip, because the expansion is delayed around the hub of the swept vane. Therefore, it could be confirmed that combustion is promoted and it became the temperature rise.

From the above results, we can conclude that a negative sweep angle at both of the hub and the tip can suppress the vane surface temperature rise.

CONCLUDING REMARKS

Three-dimensional numerical simulations were conducted for a transonic turbine stator, in order to investigate the influence of vane sweep on hydrogen combustion, surface temperature and aerodynamic performance. The most significant insights are as follows;

(1) Streamlines deflect from the hub to the tip around the leading edge and slightly deflect from the tip to the hub around the trailing edge.
(2) The vane sweep restrains the secondary flow near the hub and promotes it near the tip.
(3) The swept vane with a positive sweep angle can decrease total pressure loss.
(4) The swept vanes with a negative sweep angle can suppress static temperature rise on vane surface.
(5) The relation between the aerodynamic performance and the maximum surface temperature is trade off.

REFERENCES

[1] Brewer, G. D., 1980, “Liquid Hydrogen: Future Aircraft Fuel”, Automot. Eng., 88-8.
[2] Burnett, M. et al., 1973, “Design of a Miniature Hydrogen Fueled Gas Turbine Engine”, NASA CR-112173.

[3] Sampath, P. and Shum, F., 1985, "Combustion Performance of Hydrogen in a Small Gas Turbine Combustor", Int. J. Hydrogen Energy, 10, pp. 829-837.
[4] Hiraoka, K. et al., 1995, "Study of Internal Reheat Hydrogen Gas Turbine", Proc. IGTC1995, pp. 197-204.
[5] Nagumo, T. et al., 2000, "Numerical Investigation of Hydrogen-Fueled Combustion within Turbine Blade Passage", Proc. ISROMAC-8, 2, pp. 841-848.
[6] Nagumo, T. et al., 2001, "Three-Dimensional Computations of Hydrogen-Fueled Combustion within Turbine Blade Passage", AIAA A01-16489.
[7] Sato, M. et al., 2003, "Computation of Rotor/Stator Interaction with Hydrogen-Fuelled Combustion", ASME FEDSM2003-45618, pp. 1-6.
[8] Nagumo, T., 2003, "Geometry Optimization of Turbine Blade with Surface Injection", Proc. IGTC2003, pp. 1-7.
[9] Ikeda, J. et al., 2006, "Numerical Visualization of Combustion of Hydrogen Fuel Injected from Multiple Holes on Turbine Blade", Proc. 12th International Symposium on Flow Visualization, ISFV12-59.2, pp. 1-10.
[10] Miyama, N., 2008, "Numerical Simulation of Tip Leakage Vortex Effect on Hydrogen-Combustion Flow around 3D Turbine Blade", J. Therm. Sci., 17 (2), pp. 186-192.
[11] Denton, J. D. and Xu, L., 1999, "The exploitation of three-dimensional flow in turbomachinery design", Proc. IME C J. Mech. Eng. Sci., 213, pp. 125-137.
[12] Gotthardt, H, 1982, "Theoretische und experimentelle Untersuchen an ebenen Turbinengittern mit Pfeilung und V-stellung", Dr Ing. Dissertation, Univ. Braunschweig.
[13] Launder, B. E., and Spalding, D. B., 1974, "The Numerical Computation of Turbulent Flows", Comput. Meth. Appl. Mech. Eng., 3 (2), pp. 269-289.
[14] Huang, L. W. and Chen, C. H., 1997, "Droplet ignition in a high-temperature convective environment", Combust. Flame, 109, pp. 145-162.
[15] Balakrishnan, G. and Williams, F. A., 1994, "Turbulent combustion regimes for hypersonic propulsion employing hydrogen-air diffusion flames", J. Propul. Power, 10, pp. 434-437.
[16] Sanchez, A. L. et al., 1996, "Relationship between and Numerical Analyses for Ignition of Hydrogen-Air Diffusion Flames", Combust. Flame, 105, pp. 569-590.
[17] Chen, J. Y. et al., 1995, "Numerical simulation and scaling of NOx emissions from turbulent hydrogen jet flames with various amounts of helium dilution", Combust. Sci. and Tech., 110-111, pp. 505-529.
[18] Stull, D. R. and Propet, H., 1985, JANAF Thermochemical Tables. 3rd Edition, U. S. Dept. Commerce, Washington.
[19] Yee, H. C. and Harten, A., 1987, "Implicit TVD Schemes for Hyperbolic Conservation Laws in Curvilinear Coordinates", AIAA Journal, 3, pp. 266-274.
[20] Takahara, H. et al., 1983, "Research and Development of High Pressure Turbine", Technical Memorandum of National Aerospace Laboratory, NAL TM-484, pp. 1-28

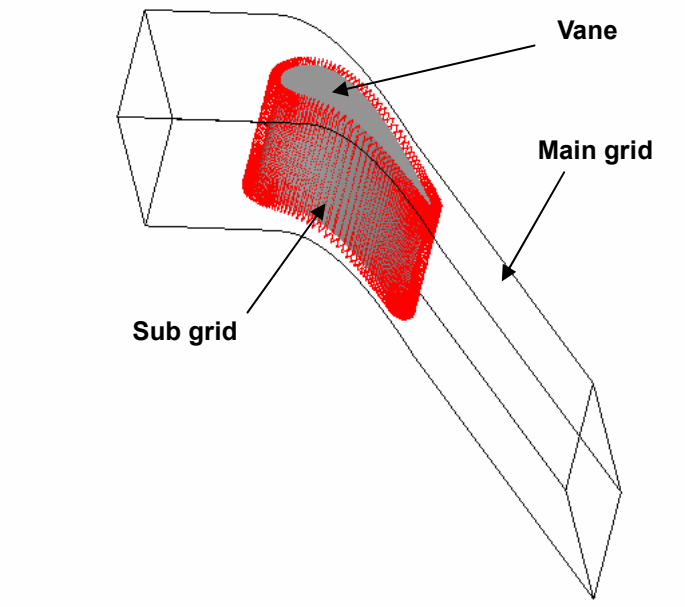

Fig. 1 Schematic of turbine cascade and computational grid

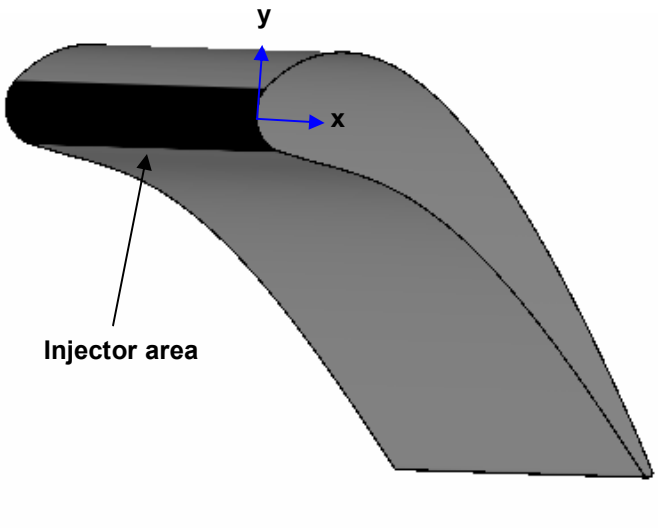

Fig. 2 Injector area

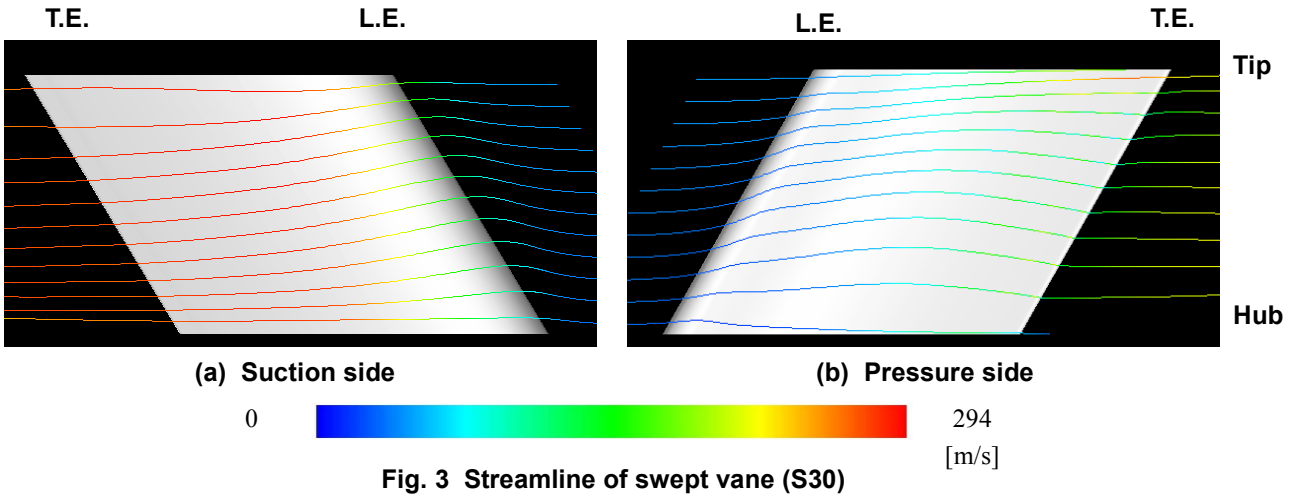

Fig. 3 Streamline of swept vane (S30)

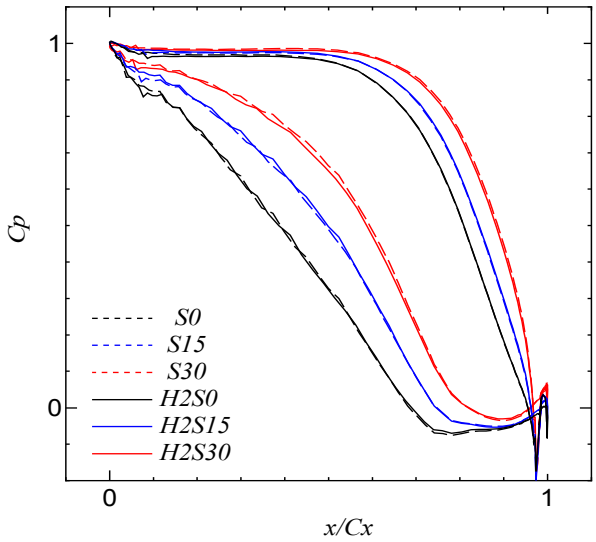

Fig. 4 Static pressure coefficient on vane surface at 5% span from hub

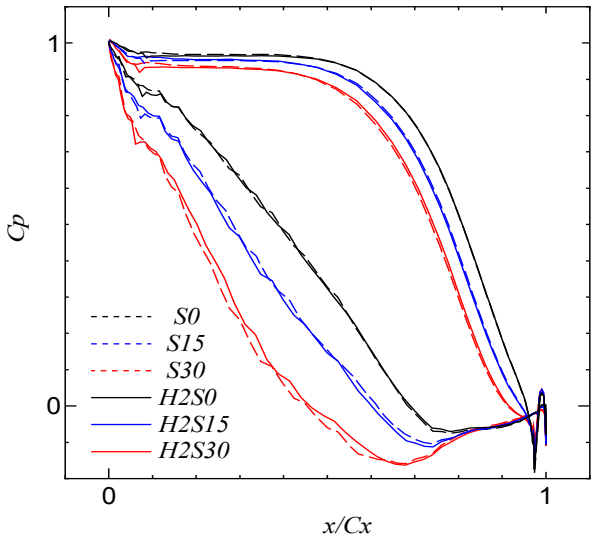

Fig. 5 Static pressure coefficient on vane surface at 5% span from tip

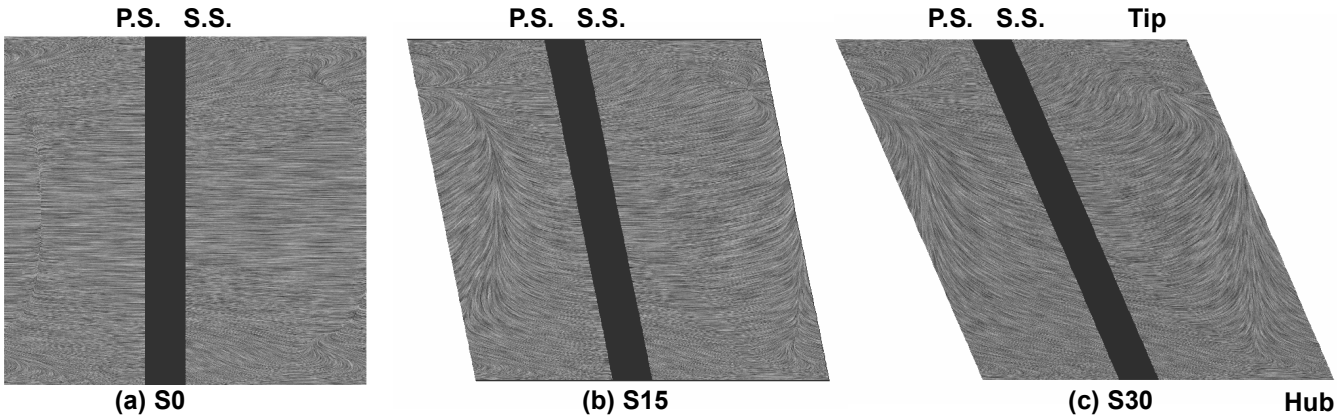

Fig. 6 Streamlines of secondary flow at 90% chord

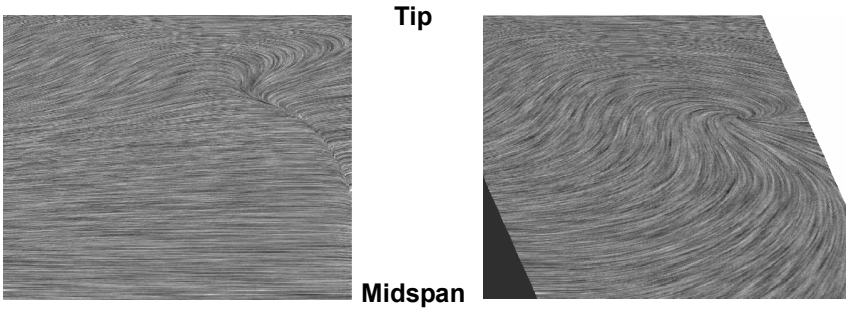

Fig. 7 Enlarged view of streamlines at 90% chord near tip

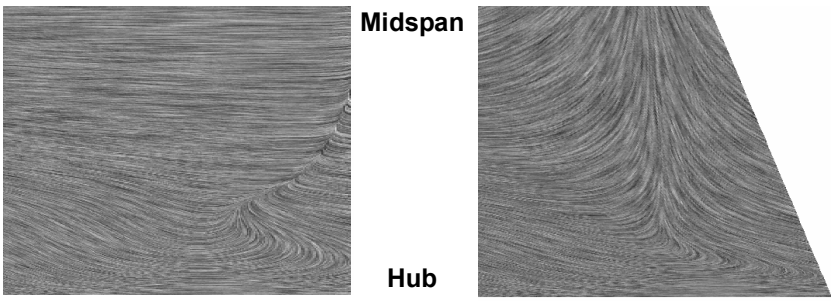

Fig. 8 Enlarged view of streamlines at 90% chord near hub

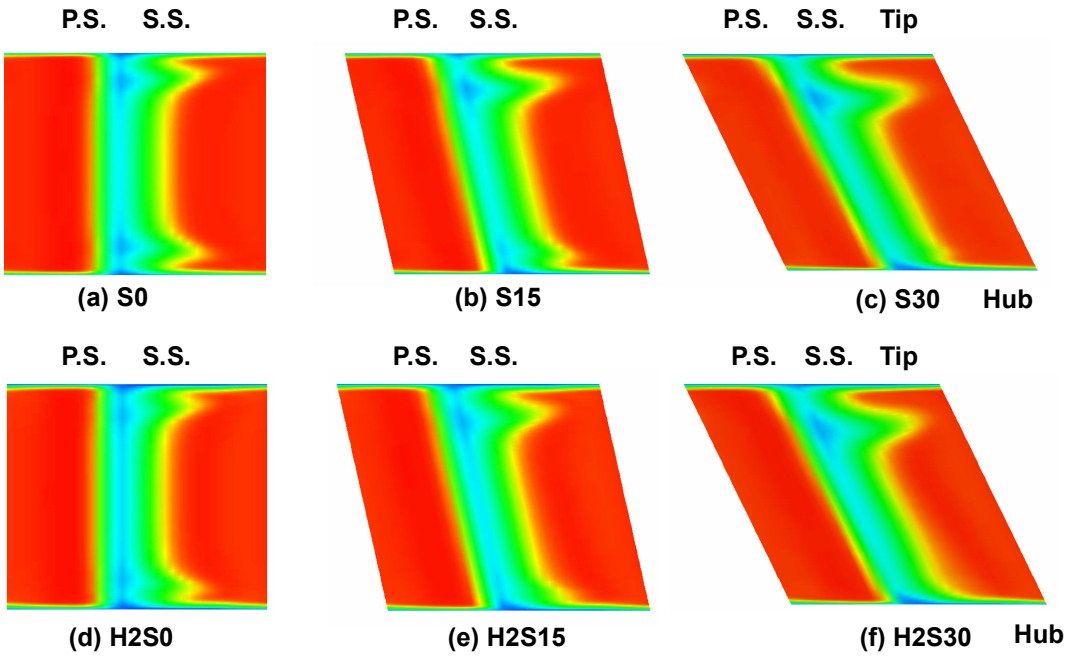

Fig. 9 Total pressure distribution at trailing edge

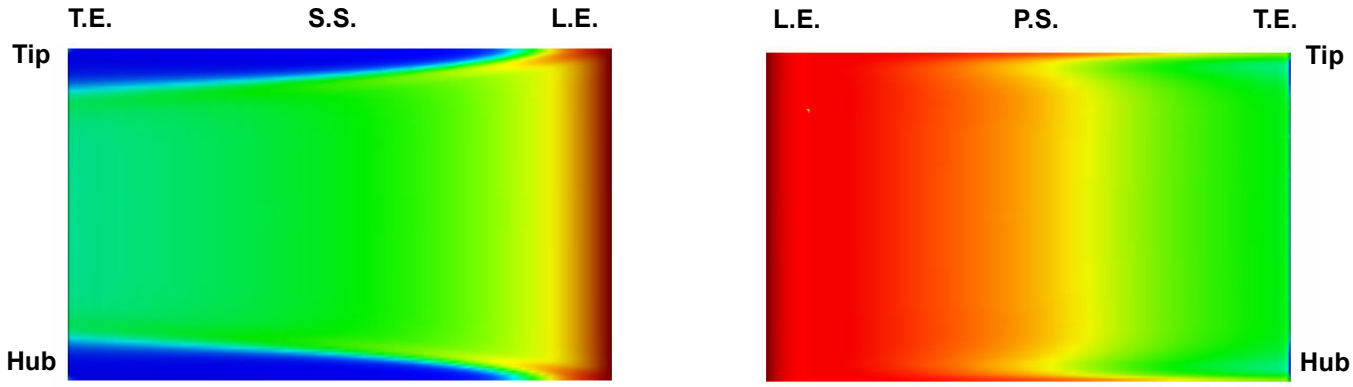

(a) H2S0

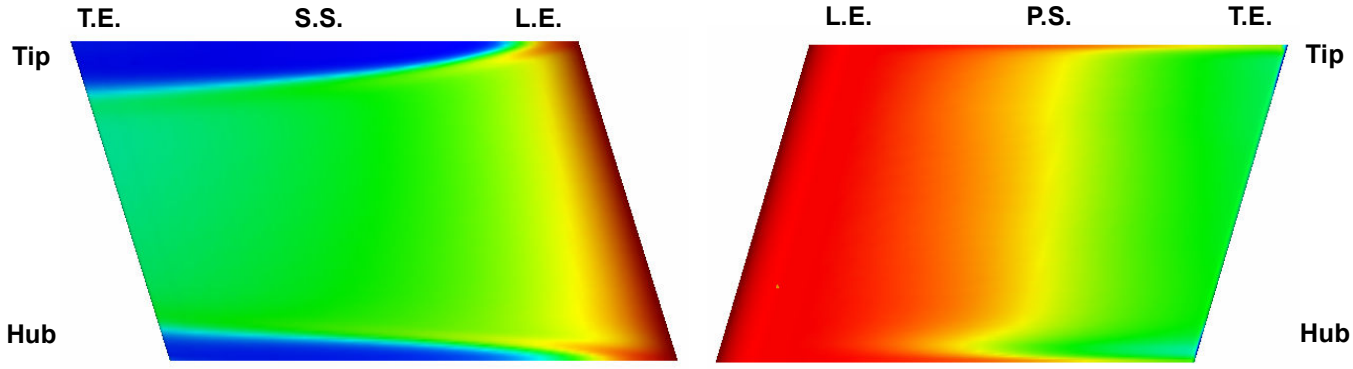

(b) H2S15

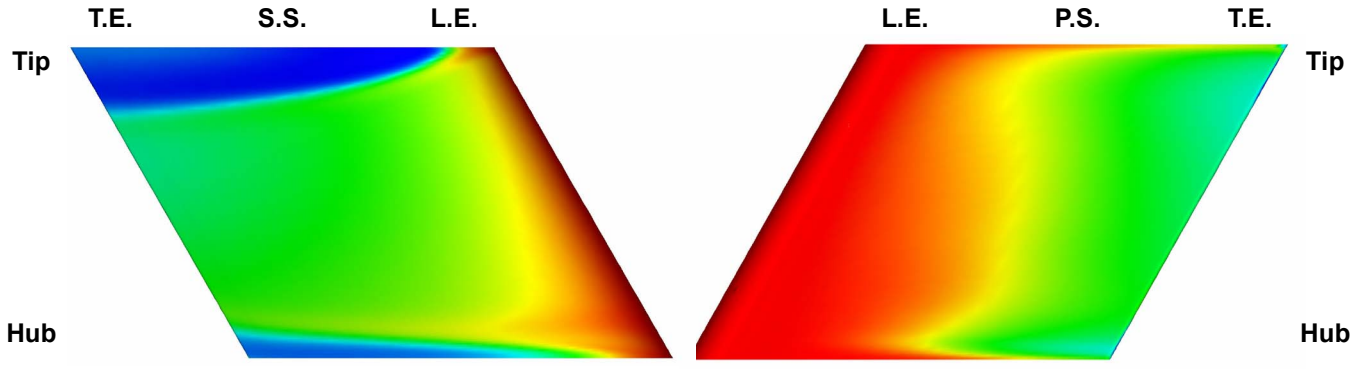

(c) H2S30

Fig. 10 H_2 mole fraction distribution on vane surface

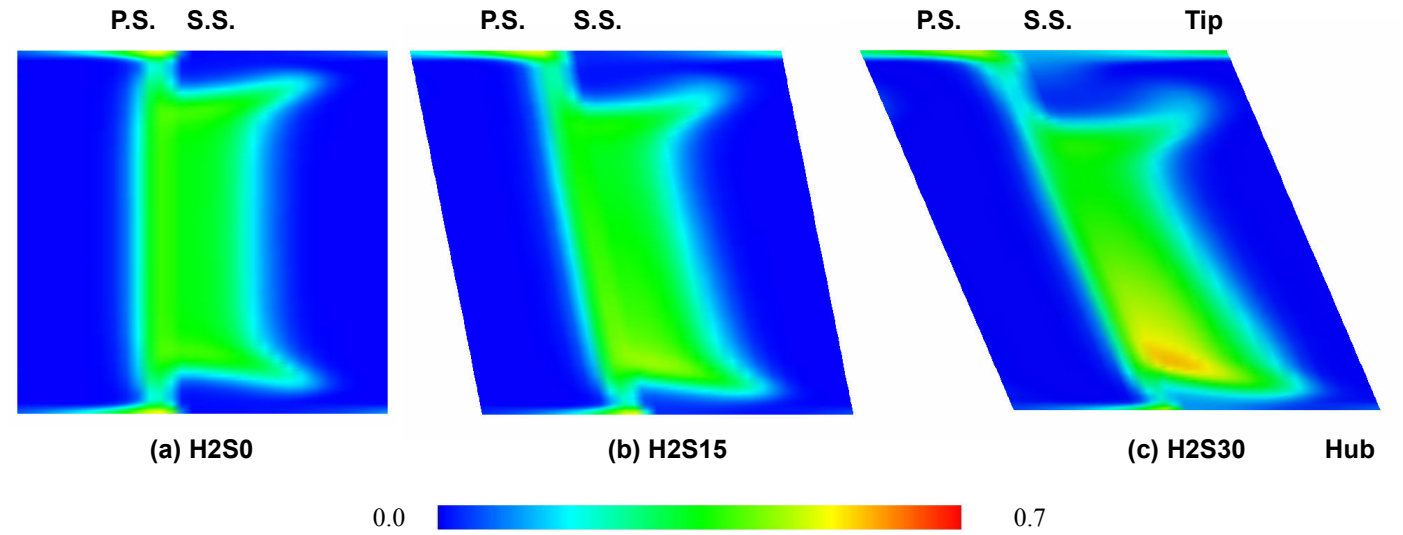

Fig. 11 H_2 mole fraction distribution at vane T.E.

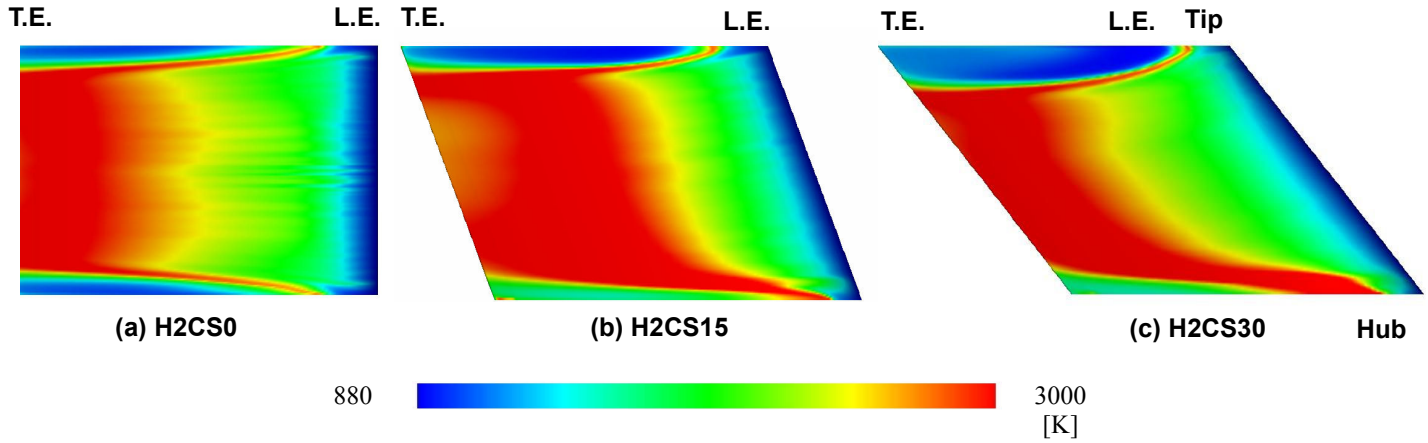

Fig. 12 Static temperature distribution on vane surface at the suction side